



ОБЪЕДИНЕННЫЙ  
ИНСТИТУТ  
ЯДЕРНЫХ  
ИССЛЕДОВАНИЙ

Дубна

00-206

E4-2000-206

A.Hamoudi, R.G.Nazmitdinov, E.Shaliev, Y.Alhassid\*

STATISTICAL FLUCTUATIONS  
OF ELECTROMAGNETIC TRANSITION INTENSITIES  
IN *pf*-SHELL NUCLEI

Submitted to «Physics Review C»

\*Center for Theoretical Physics, Sloane Physics Laboratory,  
Yale University, New Haven, Connecticut 06520, USA

2000

Random matrix theory (RMT) [1] was originally introduced to explain the statistical fluctuations of neutron resonances in compound nuclei [2]. The theory assumes that the nuclear Hamiltonian belongs to an ensemble of random matrices that are consistent with the fundamental symmetries of the system. In particular, since the nuclear interaction preserves time-reversal symmetry, the relevant ensemble is the Gaussian orthogonal ensemble (GOE). The use of RMT in the compound nucleus was justified by the complexity of the nuclear system. Bohigas *et al* [3] conjectured that RMT describes the statistical fluctuations of a quantum system whose associated classical dynamics is chaotic. RMT has become a standard tool for analyzing the universal statistical fluctuations in chaotic systems [4,5].

The chaotic nature of the single-particle dynamics in the nucleus can be studied in the mean-field approximation. The interplay between shell structure and fluctuations in the single-particle spectrum has been understood in terms of the classical dynamics of the nucleons in the corresponding deformed mean-field potential [6,7]. However, the residual nuclear interaction mixes different mean-field configurations and affects the statistical fluctuations of the many-particle spectrum and wavefunctions. Various nuclear structure models can be used to study these fluctuations. The statistics of the low-lying collective part of the nuclear spectrum have been studied in the framework of the interacting boson model, in which the nuclear fermionic space is mapped onto a much smaller space of bosonic degrees of freedom [8,9]. Because of the relatively small number of degrees of freedom in this model, it was also possible to relate the statistics to the underlying mean-field collective dynamics. At higher excitations additional degrees of freedom (such as broken pairs) become important [10], and the effects of interactions on the statistics must be analyzed in larger model spaces. The interacting shell model offers an attractive framework for such studies where realistic effective interactions are available and where the basis states are labeled by exact quantum numbers of angular momentum, isospin and parity [11].

RMT makes definite predictions for the statistical fluctuations of both the eigenfunctions and the spectrum. The electromagnetic transition intensities in a nucleus are observables that are sensitive to the wavefunctions, and the study of their statistical distributions should

complement [8,9] the more common spectral analysis. Using the interacting shell model,  $B(M1)$  and  $B(E2)$  transitions were recently analyzed in  $^{22}\text{Na}$  [12] and found to follow the Porter-Thomas distribution [13], in agreement with RMT and consistent with the previous finding of a Gaussian distribution for the eigenvector components [14]- [17].

Most studies of statistical fluctuations in the shell model have been restricted to lighter nuclei ( $A \lesssim 40$ ) where complete  $0\hbar\omega$  calculations are feasible (e.g.  $sd$ -shell nuclei). It is of interest to investigate the statistics in other mass regions. In this paper we study the fluctuation properties of  $\Delta T = 0$  electromagnetic transition intensities in nuclei with  $A \sim 60$ . We find that  $B(E2)$  as well as  $\Delta J \neq 0$   $B(M1)$  intensities are described by the Porter-Thomas distribution, but that the  $\Delta T = \Delta J = 0$   $M1$  statistics are sensitive to  $T_z$  and show a significant deviation from a Porter-Thomas distribution in self-conjugate nuclei

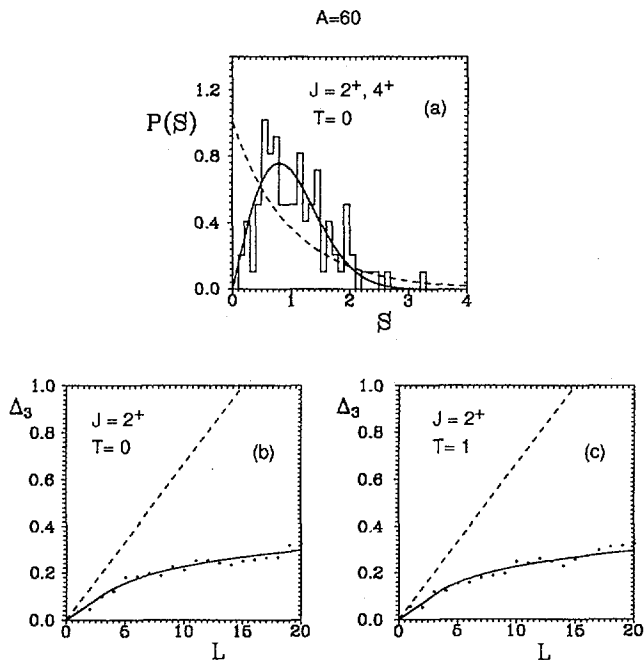


FIG. 1. Spectral statistics in  $A = 60$  nuclei. (a) Nearest-neighbor level spacing distribution  $P(s)$  for  $T = 0$  states with  $J = 2, 4$  (histograms). The solid line is the Wigner-Dyson distribution and the dashed line is the Poisson distribution. Bottom:  $\Delta_3$ -statistic for  $J = 2$  levels with (b)  $T = 0$  and (c)  $T = 1$ . Also shown are the GOE (solid lines) and Poisson (dashed lines) limits.

( $T_z = 0$ ). At the same time the spectral statistics are found to be fully consistent with RMT (at a given spin and isospin). Since full  $pf$ -shell calculations are currently not feasible for  $A \sim 60$  nuclei, we perform  $pf$ -shell calculations with  $^{56}\text{Ni}$  as a core, i.e., we assume a fully occupied  $f_{7/2}$  orbits and consider all possible many-nucleon configurations defined by the  $0f_{5/2}$ ,  $1p_{3/2}$  and  $1p_{1/2}$  orbitals. The effective interaction is chosen to be the isospin-conserving F5P interaction [18]. This interaction is successful in describing the mass range  $A \sim 57 - 68$ . The calculations were performed using the shell model program OXBASH [19].

To test the validity of RMT in the above model space, we first study the spectral fluctuations for states with good spin and isospin. Fig. 1(a) shows the nearest-neighbors level spacing distribution  $P(s)$  for the unfolded  $T = 0$  levels. To improve the statistics we combine the spacings of the  $J = 2$  states and those of the  $J = 4$  states. The calculated distribution (histograms) is in agreement with the Wigner-Dyson distribution (solid line), and level repulsion is clearly observed at small spacings. The Poisson distribution, which corresponds to a random sequence of levels (and characterizes regular systems), is shown by the dashed line for comparison. Another measure of fluctuations is the spectral rigidity described by Dyson's  $\Delta_3$  statistic [1]. The bottom panels of Fig. 1 show  $\Delta_3(L)$  versus  $L$  for  $J = 2$  states with  $T = 0$  (panel (b)) and  $T = 1$  (panel (c)). The results agree well with the GOE limit (solid lines).

We now consider the electromagnetic transitions intensities. Denoting by  $B(\bar{\omega}L; i \rightarrow f)$  the reduced transition probability from an initial state  $|i\rangle$  to a final state  $|f\rangle$ , with  $\bar{\omega}$  indicating the electric ( $E$ ) or magnetic ( $M$ ) character of the transition, and  $2^L$  the multipolarity, we have [20]

$$B(\bar{\omega}L; J_i T_i T_z \rightarrow J_f T_f T_z) = \frac{|\delta_{T_i T_f} M_{is}(\bar{\omega}L) - (T_i T_z 10 | T_f T_z) M_{iv}(\bar{\omega}L)|^2}{(2J_i + 1)(2T_i + 1)}. \quad (1)$$

Here  $M_{is}(\bar{\omega}L)$  and  $M_{iv}(\bar{\omega}L)$  are the triply reduced matrix elements for the isoscalar and isovector components of the transition operator, respectively. Note that these matrix elements depend on  $J_i, T_i$  and  $J_f, T_f$  but not on  $T_z$ . For  $\Delta T = 0$  transitions ( $T_i = T_f = T$ ) the isospin Clebsch-Gordan coefficient in Eq. (1) is simply given by

$$(TT_z 10 | TT_z) = T_z / \sqrt{T(T+1)}. \quad (2)$$

It follows that the isovector component in Eq. (1) is absent for self-conjugate (i.e.  $T_z = 0$ )

nuclei. Thus the statistics of the isoscalar component of an electromagnetic transition operator can be inferred directly from the study of  $\Delta T = 0$  transitions in  $T_x = 0$  nuclei. Consequently, we are able to test the sensitivity of the statistics to the isovector and the isoscalar contributions. Below we present results for E2 and M1 transitions. The E2 transitions were calculated using standard effective charges of  $e_p = 1.5$  and  $e_n = 0.5$ . We note, however, that the isoscalar and isovector components of E2 are (up to a proportionality constant) independent of the effective charges, and their corresponding statistics are thus also independent of the particular choice of effective charges.

To study the fluctuation properties of the transition rates, it is necessary to divide out any secular variation of the average strength function versus the initial and final energies. We calculate an average transition strength at an initial energy  $E$  and final energy  $E'$  from [21,9]

$$\langle B(\bar{\omega}L; E, E') \rangle = \frac{\sum_{i,f} B(\bar{\omega}L; i \rightarrow f) e^{-(E-E_i)^2/2\gamma^2} e^{-(E'-E_f)^2/2\gamma^2}}{\sum_{i,f} e^{-(E-E_i)^2/2\gamma^2} e^{-(E'-E_f)^2/2\gamma^2}}, \quad (3)$$

where  $\gamma$  is a parameter chosen as described below. For fixed values of the initial ( $J_i^T, T$ ) and final ( $J_f^T, T$ ) spin/parity and isospin, we calculate from Eq. (1) the intensities  $B(\bar{\omega}L; i \rightarrow f)$ . All transitions of a given operator (e.g. M1 or E2) between the initial and final states of the given spin/parity and isospin classes have been included in the statistics. We remark that the energy levels used in (3) are the unfolded energy levels [22], characterized by a constant mean spacing. The value of  $\gamma$  in (3) has been chosen to be large enough to minimize effects arising from the local fluctuations in the transition strength but not so large as to wash away the secular energy variation of the average intensity. In the present calculations we used  $\gamma \sim 2.5$ . We renormalized the actual intensities by dividing out their smooth part

$$y_{fi} = \frac{B(\bar{\omega}L; J_i^T T_z \rightarrow J_f^T T_z)}{\langle B(\bar{\omega}L; E, E') \rangle}, \quad (4)$$

and construct their distribution using bins that are equally spaced in  $\log y$ . In RMT there is a large number of weak transitions, and we use  $\log y$  as the variable in order to display small values of  $y$  (over several orders of magnitude). For each transition operator and each class of initial and final states we fit to the calculated distribution a  $\chi^2$  distribution in  $\nu$  degrees of freedom [23]

$$P_\nu(y) = (\nu/2 < y >)^{\nu/2} y^{\nu/2-1} e^{-\nu y/2 < y >} / \Gamma(\nu/2). \quad (5)$$

For  $\nu = 1$  this distribution reduces to the Porter-Thomas distribution. In systems with mixed classical dynamics, it is found that  $\nu$  decreases monotonically from 1 as the system makes a transition from chaotic to regular motion [21].

We first examine all  $E2$  and  $M1$   $2^+, T \rightarrow 2^+, T$  transitions ( $T = 0$  or  $T = 1$ ) in  $A = 60$  nuclei.  $T = 0$  states exist only in  $T_z = 0$  nuclei, i.e.,  $^{60}\text{Zn}$  in our case. However, the  $T = 1$  states form isobaric multiplets in  $^{60}\text{Co}$ ,  $^{60}\text{Zn}$  and  $^{60}\text{Cu}$ . In the latter case we studied the statistics in both  $T_z = 0$  and  $T_z = 1$  nuclei. Because of the vanishing of the isovector Clebsch-Gordan coefficient in Eq. (1), the transitions in  $^{60}\text{Zn}$  ( $T_z = 0$ ) are purely isoscalar. For each transition operator we sampled  $56^2 = 3136$  and  $66^2 = 4356$  matrix elements for  $T = 0$  and  $T = 1$ , respectively. The calculated distributions (histograms) of the  $B(E2)$  (left panels) and  $B(M1)$  (right panels)  $2^+, T \rightarrow 2^+, T$  transitions are shown in Fig. 2, and compared with the Porter-Thomas distribution (Eq. (5) with  $\nu = 1$ ). The distributions of

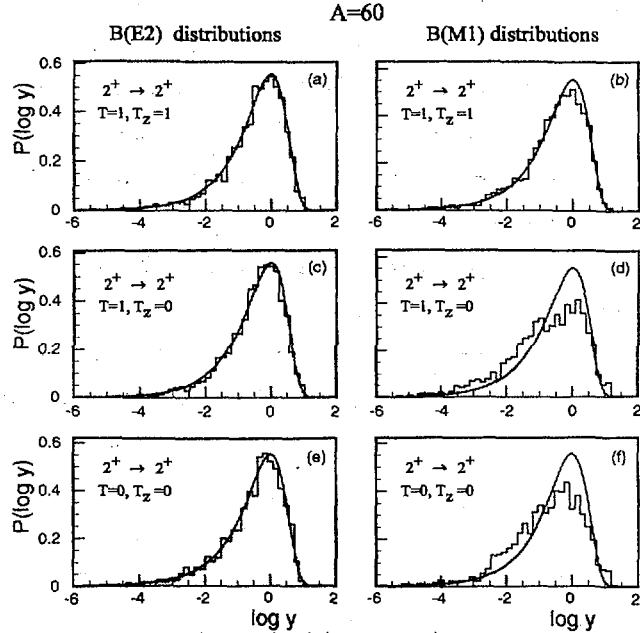


FIG. 2. The  $B(E2)$  (left panels) and  $B(M1)$  (right panels) intensity distributions (histograms) for the  $2^+, T \rightarrow 2^+, T$  transitions in  $A = 60$  nuclei: (a,b)  $2^+, 1 \rightarrow 2^+, 1$  transitions ( $T_z = 1$ ); (c,d)  $2^+, 1 \rightarrow 2^+, 1$  transitions ( $T_z = 0$ ); (e,f)  $2^+, 0 \rightarrow 2^+, 0$  transitions ( $T_z = 0$ ). The solid lines describe the Porter-Thomas distribution (Eq. (5) with  $\nu = 1$ ). Notice the deviation from Porter-Thomas statistics in (d) and (f).

transitions within the  $T = 1$  states are shown in the top ( $T_z = 1$ ) and middle ( $T_z = 0$ ) panels. Since our interaction is isospin invariant, the energy levels of an isobaric multiplet are degenerate, and the spectral statistics of  $T = 1$  states must be the same in both  $T_z = 0$  and  $T_z = 1$  nuclei. As discussed earlier these levels display GOE statistics (see Fig. 1). However, while the  $B(E2)$  distributions are all in agreement with the GOE prediction, the  $M1$  distributions are sensitive to  $T_z$ . For  $T_z = 1$  nuclei the distribution of the  $M1$  intensities is Porter-Thomas (Fig. 2b), but in self-conjugate nuclei ( $T_z = 0$ ) we find that the  $M1$  distribution deviates significantly from the GOE limit (Fig. 2d). Since various transition operators probe different components of the wavefunctions, it is possible that deviation from the statistical limit will occur for some of these operators. Such a deviation from a Porter-Thomas distribution suggests that some approximate selection rules might still be effective in an otherwise statistical regime [23]. A deviation from the RMT limit is also observed in the  $M1$  distribution for the  $2^+, T = 0 \rightarrow 2^+, T = 0$  transitions (Fig. 2f), while the  $B(E2)$  probabilities are distributed according to Porter-Thomas (Fig. 2e). In both cases (i.e.  $T = 0$  and  $T = 1$ ) the deviation from the GOE limit occurs for the  $M1$  transitions in self-conjugate nuclei (e.g.  $^{60}\text{Zn}$ ), where the matrix elements are purely isoscalar. In  $T_z = 1$  nuclei, both isoscalar and isovector components contribute to the  $M1$  transitions. However, since the isoscalar  $M1$  matrix elements are much weaker than the isovector  $M1$  [20], the latter dominate and the distributions are restored to their GOE form.

To check that our conclusion does not depend on the size of the model space, we performed similar calculations in a model space with 6 active particles, i.e., for  $A = 62$  nuclei. The results are shown in Fig. 3. Again, we observe that the distributions of the  $M1$  transitions in the self-conjugate nucleus  $T_z = 0$  (i.e.,  $^{62}\text{Ga}$ ) deviate from Porter-Thomas (Fig. 3d,f).

Our conclusions are not restricted to the  $pf$ -shell. Adams *et al* [12] calculated the distributions of electromagnetic transitions for the  $N = Z$  ( $T_z = 0$ ) nucleus  $^{22}\text{Na}$  in the  $sd$ -shell (where the number of active nucleons is 6), and found Porter-Thomas distributions for both  $E2$  and  $M1$  transitions. However, the  $M1$  distribution they show includes contributions from both isoscalar and isovector transitions. In Fig. 5 we show distributions of the  $1^+, T \rightarrow 1^+, T$  transitions in two  $A = 22$  nuclei:  $^{22}\text{Ne}$  ( $T_z = 1$ ) and  $^{22}\text{Na}$  ( $T_z = 0$ ). Similarly to our results in the  $pf$ -shell, we see deviations from the Porter-Thomas distribution for the purely

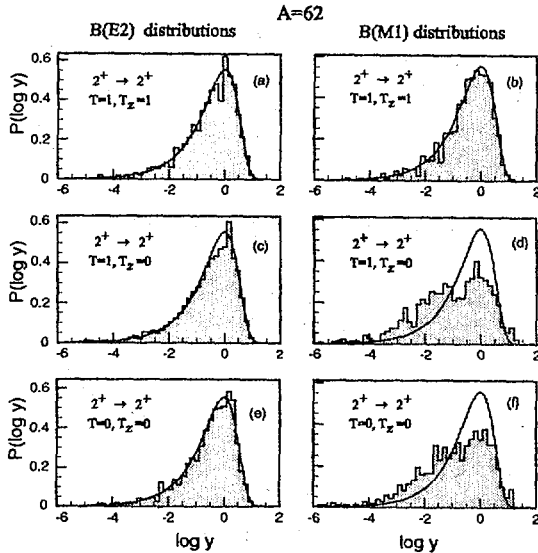


FIG. 3. As in Fig.2 but for  $A = 62$  nuclei.

isoscalar  $M1$  transitions between states with selection rules  $\Delta J = \Delta T = 0$  in the self-conjugate nucleus  $^{22}\text{Na}$  (Fig. 4(d),(f)).

The deviations from Porter-Thomas statistics are seen only for the isoscalar  $M1$  transitions between states with  $\Delta J = 0$ . The  $\Delta J = 1$  isoscalar  $M1$  transitions satisfy the RMT statistics as can be seen in Fig. 5(a),(b) for  $A = 60$  and  $A = 62$   $T_z = 0$  nuclei.

The  $M1$  operator is composed of orbital and spin parts. The isoscalar  $M1$  is particularly simple and can be written (in units of nuclear magneton  $\mu_N$ ) as

$$\frac{g_p^l + g_n^l}{2} \mathbf{L} + \frac{g_p^s + g_n^s}{2} \mathbf{S}, \quad (6)$$

where  $\mathbf{L}$  and  $\mathbf{S}$  are the total orbital angular momentum and spin, respectively, and  $g_{p,n}^l$ ,  $g_{p,n}^s$  are the proton and neutron orbital and spin  $g$  factors. Since the transition matrix elements of the total angular momentum  $\mathbf{J} = \mathbf{L} + \mathbf{S}$  between different states vanish, the orbital and spin contributions to the isoscalar  $M1$  matrix elements always have opposite signs. Consequently, the off-diagonal elements are small. However, the  $\Delta J = 0$  transitions



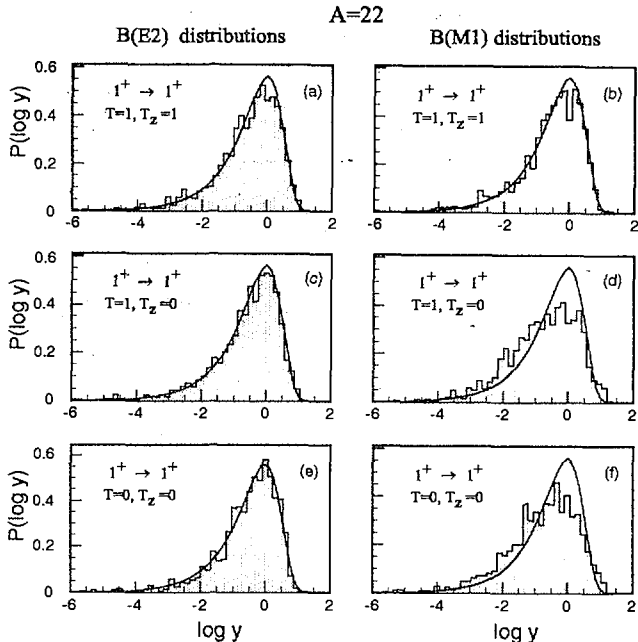


FIG. 4. As in Fig.2 but for  $A = 22$  nuclei.

include diagonal matrix elements where the interference between the orbital and spin can be constructive, leading to larger matrix elements. The combination of a small number of large matrix elements and many small matrix elements can explain the deviation from the Porter-Thomas statistics. Indeed we have verified that a Porter-Thomas distribution is recovered (see Fig. 5(c),(d)) when only off-diagonal matrix elements are included in the analysis. In the case of the isovector  $M1$  matrix elements, the relative phase of the orbital and spin contributions is more random [24], and the corresponding statistics are Porter-Thomas.

In conclusion, we have studied  $\Delta T = 0$   $B(E2)$  and  $B(M1)$  transition strength distributions in  $pf$ -shell nuclei with  $A = 60, 62$ . While most of the calculated distributions are in close agreement with the Porter-Thomas distribution predicted by the GOE, we find that the  $\Delta J = 0$   $M1$  transitions in self-conjugate nuclei ( $T_z = 0$ ) deviate from the RMT limit. For these nuclei the  $M1$  transitions are purely isoscalar and relatively weak compared with  $M1$  transitions in  $T_z = 1$  nuclei, which are dominated by the isovector component of  $M1$ .

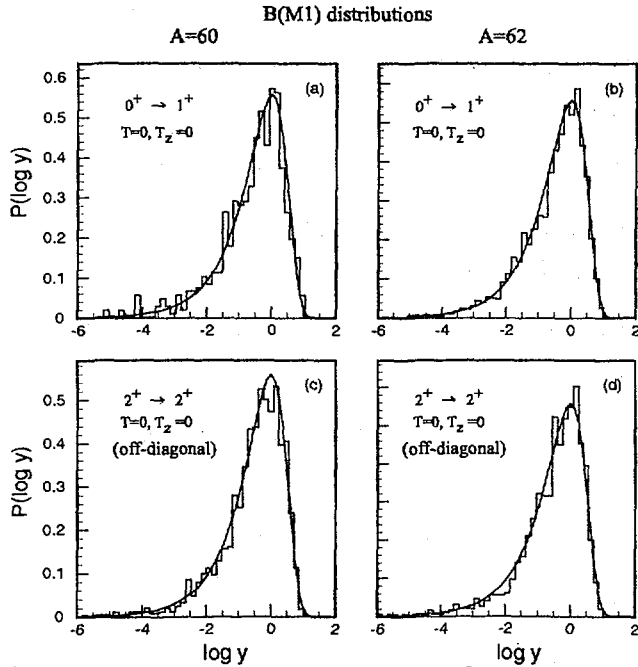


FIG. 5.  $B(M1)$  intensity distributions for isoscalar  $T = 0 \rightarrow T = 0$  transitions in  $A = 60$  (left panels) and  $A = 62$  (right panels)  $T_z = 0$  nuclei: (a,b)  $0^+ \rightarrow 1^+$  transitions; (c, d) off-diagonal  $2^+ \rightarrow 2^+$  transitions.

Similar deviations of the  $\Delta J = 0$  isoscalar  $M1$  distribution from Porter-Thomas statistics are observed in  $sd$ -shell nuclei, indicating that this is likely a generic effect.

This work was supported in part by the Department of Energy grant No. DE-FG-0291-ER-40608 and by the Russian Foundation for Basic Research, project No. 00-02-17194 and grand No. 97-27-15L with project 96-15-96423.

## REFERENCES

- [1] M.L. Mehta, *Random Matrices* 2nd ed. (Academic Press, New York, 1991).
- [2] C.E. Porter, *Statistical Theories of Spectra: Fluctuations* (Academic Press, New York, 1965).

- [3] O. Bohigas, M.J. Giannoni and C. Schmit, Phys. Rev. Lett. **52**, 1 (1984).
- [4] T.A. Brody, J. Flores, J.B. French, P.A. Mello, A. Pandey and S.S.M. Wong, Rev. Mod. Phys. **53**, 385 (1981).
- [5] T. Guhr, A. Müller-Groeling and H.A. Weidenmüller, Phys. Rep. **299**, 189 (1998).
- [6] W.D. Heiss, R.G. Nazmitdinov and S. Radu, Phys. Rev. Lett. **72**, 2351 (1994); Phys. Rev. C **52**, R1179 (1995); Phys. Rev. C **52**, 3032 (1995).
- [7] W.D. Heiss, R.A. Lynch and R.G. Nazmitdinov, JETP Lett. **69**, 563 (1999); Phys. Rev. C **60**, 034303 (1999).
- [8] Y. Alhassid, A. Novoselsky and N. Whelan, Phys. Rev. Lett. **65**, 2971 (1990); Y. Alhassid and N. Whelan, Phys. Rev. C **43**, 2637 (1991).
- [9] Y. Alhassid and A. Novoselsky, Phys. Rev. C **45**, 1677 (1992).
- [10] Y. Alhassid and D. Vretenar, Phys. Rev. C **46**, 1334 (1992).
- [11] V. Zelevinsky, B.A. Brown, N. Frazier and M. Horoi, Phys. Rep. **276**, 87 (1996).
- [12] A.A. Adams, G.E. Mitchell, W.E. Ormand and J.F. Shrinier Jr., Phys. Lett. B **392**, 1 (1997).
- [13] C.E. Porter and R.G. Thomas, Phys. Rev. **104**, 483 (1956).
- [14] R.R. Whitehead, A. Watt, D. Kelvin and A. Conkie, Phys. Lett. B **76**, 149 (1978).
- [15] J.J.M. Verbaarschot and P.J. Brussaard, Phys. Lett. B **87**, 155 (1979).
- [16] B.A. Brown and G.F. Bertsch, Phys. Lett. B **148**, 5 (1984).
- [17] H. Dias, M.S. Hussein, N.A. de Oliveira and B.H. Wildenthal, J. Phys. G **15**, L79 (1989).
- [18] P.W.M. Glaudemans, P.J. Brussaard and R.H. Wildenthal, Nucl. Phys. A **102**, 593 (1976).
- [19] B.A. Brown, A. Et'chegoyen and W.D.M Rae, the OXBASH shell model code, MSUCL Report No. 524 (1988).
- [20] P.J. Brussaard and P.W.M. Glaudemans, *Shell- model applications in nuclear spectroscopy* (North Holland, Amsterdam, 1977).

- [21] Y. Alhassid and M. Feingold, Phys. Rev. A **39**, 374 (1989).
- [22] O. Bohigas and M.J. Giannoni, in *Mathematical and Computational Methods in Nuclear Physics*, edited by J.S. Dehesa, J.M. Gomes and A. Polls (Springer Verlag, New York, 1983).
- [23] Y. Alhassid and R.D. Levine, Phys. Rev. Lett. **57**, 2879 (1986).
- [24] M.S. Fayache, L. Zamick, Y.Y. Sharon and Y. Durga Devi, Phys.Rev. C **61**, art. no. 024308 (2000).

**Received by Publishing Department  
on September 4, 2000.**